

Functional Clustering for Longitudinal Associations between Social Determinants of Health and Stroke Mortality in the US

Fangzhi Luo^{*†}, Jianbin Tan[‡], Donglan Zhang[§], Hui Huang[¶] and Ye Shen^{||}

Abstract

Understanding the longitudinally changing associations between Social Determinants of Health (SDOH) and stroke mortality is essential for effective stroke management. Previous studies have uncovered significant regional disparities in the associations between SDOH and stroke mortality. However, existing studies have not utilized longitudinal associations to develop data-driven methods for regional division in stroke control. To fill this gap, we propose a novel clustering method to analyze SDOH-stroke mortality associations across U.S. counties. To enhance the interpretability of the clustering outcomes, we introduce a novel regularized expectation-maximization algorithm equipped with sparsity- and smoothness-pursued penalties, aiming at simultaneous clustering and variable selection in longitudinal associations. As a result, we can identify key SDOH that contributes to longitudinal changes in stroke mortality. This facilitates the clustering of U.S. counties based on the associations between these SDOH and stroke mortality. The effectiveness of our proposed method is demonstrated through extensive numerical studies. By applying our method to longitudinal data on SDOH and stroke mortality at the county level, we identify 18 important SDOH for stroke mortality and divide the U.S. counties into two clusters based on these selected SDOH. Our findings unveil complex regional heterogeneity in the longitudinal associations between SDOH and stroke mortality, providing valuable insights into region-specific SDOH adjustments for mitigating stroke mortality.

Keywords: Model-based clustering, Functional regression model, Variable selection, Regularized expectation-maximization algorithm, Stroke mortality

^{*}Department of Epidemiology and Biostatistics, College of Public Health, University of Georgia, Athens, GA, USA. The authors gratefully acknowledge *the National Natural Science Foundation of China (grants nos. 12292980, 12292984 and 12231017)* and *the MOE project of key research institute of humanities and social sciences (grant no. 22JJD910001)*.

[†]Jianbin Tan is the co-first author.

[‡]Department of Biostatistics and Bioinformatics, School of Medicine, Duke University, Durham, NC, USA.

[§]Department of Foundations of Medicine, NYU Grossman Long Island School of Medicine, Mineola, NY, USA.

[¶]Center for Applied Statistics and School of Statistics, Renmin University of China, Beijing, China

^{||}Department of Epidemiology and Biostatistics, College of Public Health, University of Georgia, Athens, GA, USA.

1 Introduction

The burden of stroke in the United States is enormous. As one of the most prevalent cardiovascular diseases, stroke remains consistently among the top five causes of death in the country ([Koton et al. \(2014\)](#)), leading to over 130,000 fatalities annually ([Holloway et al. \(2014\)](#)). In the effort to prevent stroke deaths, Social Determinants of Health (SDOH)—encompassing economic, social, and environmental conditions where people live, learn, work, and play ([Havranek et al. \(2015\)](#))—have garnered significant attention due to their strong associations with stroke mortality ([Reshetnyak et al. \(2020\)](#); [Skolarus et al. \(2020\)](#); [Powell-Wiley et al. \(2022\)](#)). In 2013, Centers for Disease Control and Prevention (CDC) released an important report on health disparities ([Frieden et al. \(2013\)](#)), where the relationships between SDOH and stroke mortality were extensively documented. In 2015, the impact of SDOH on stroke mortality was highlighted in an important scientific statement by the American Heart Association (AHA) ([Mozaffarian et al. \(2015\)](#)). Since 2019, the AHA has consistently emphasized the importance of SDOH in its Annual Heart Disease and Stroke Statistics Report, spanning across all chapters ([Benjamin et al. \(2019\)](#)). These declarations underscore the urgency of understanding the associations between SDOH and stroke mortality. This understanding is crucial for informing targeted interventions aimed at controlling stroke mortality by addressing underlying social, economic, and environmental factors.

Recent findings have revealed a clear regional disparity in the associations between SDOH and stroke mortality. For instance, [Zelko et al. \(2023\)](#) identified statewide differences in these associations. Additionally, [Villablanca et al. \(2016\)](#) and [Son et al. \(2023\)](#) observed significant disparities in the associations between rural and urban areas. To address such regional disparities, various statewide ([Gebreab et al. \(2015\)](#)) and rural-urban strategies ([Labarthe et al. \(2014\)](#); [Record et al. \(2015\)](#); [Kapral et al. \(2019\)](#)) have been developed for region-specific stroke management. However, the existing literature primarily adopts prespecified regional division strategies when analyzing regional disparities, which do not guarantee that areas within a divided region share similar associations between SDOH and stroke mortality. This can potentially lead to ineffective regional division strategies for stroke control. Moreover, many SDOH exhibit longitudinal changes in their associations with stroke mortality ([He et al. \(2021\)](#); [Imoisili \(2024\)](#)), a factor crucial for timely policymaking in stroke management. Targeting these longitudinal as-

sociations, clustering becomes a vital tool for determining reasonable regional divisions in stroke prevention. Nevertheless, this remains an unsolved issue that requires further investigation.

In this work, we propose a novel method for clustering longitudinal associations between SDOH and stroke mortality. Generally, the clustering is implemented based on the similarity among SDOH-stroke mortality associations across counties in the U.S., and the resulting clustering outcomes can inform region-specific prevention measures for controlling stroke mortality. To achieve this, we utilize county-level longitudinal data on SDOH and stroke mortality in the U.S., treating the longitudinally observed data in each county as functional data (Ramsay and Silverman (2005); Wang et al. (2016)). Consequently, the concurrent associations between SDOH and stroke mortality are inherently functional objects, which can be effectively modeled using functional regression models (Yao et al. (2005); Wang et al. (2008); Zhu et al. (2012); Morris (2015); Kong et al. (2016); Zhou et al. (2023)), where the coefficients are also functional, capturing the relationship between SDOH and stroke mortality over time. For the clustering process, we model these functional coefficients using a finite mixture model, leading to a finite mixture of functional regression models. This approach enables the clustering of U.S. counties into different regions based on the relationship between their SDOH and stroke mortality.

Related Literature Our task essentially differs from the common clustering procedures for longitudinal data (Chiou and Li (2007); Peng and Müller (2008); McNicholas and Murphy (2010); Jacques and Preda (2013); Komárek and Komárková (2013); Jacques and Preda (2014); Tang and Qu (2016)), which primarily apply to observable longitudinal outcomes. In contrast, the county-level longitudinal associations between SDOH and stroke mortality in our study are unobservable. To cluster these associations, one might consider applying finite mixtures of regression models (Peel and MacLahlan (2000); Khalili and Chen (2007); Khalili and Lin (2013)) to the SDOH and stroke mortality longitudinal data. However, this approach does not account for longitudinal changes in the associations within the clustering procedures, which could lead to unreliable clustering outcomes due to the disregard of longitudinal signals.

In light of functional data analysis (Ramsay and Silverman (2002, 2005); Wang et al. (2016)), some studies proposed a finite mixture of functional regression models (Yao et al. (2011); Lu and Song (2012); Wang et al. (2023)) to account for time-varying changes

within mixture regression models. However, these methods do not address the issue of collinearity among covariates within their regression models. In our case, the collection of SDOH served as functional covariates, exhibits significant collinearity due to their derivation from multiple domains (e.g., social, economic, and environmental domains). Ignoring collinearity among the SDOH data may lead to misspecification in the functional regression model, potentially compromising the accuracy of the resultant clustering outcome.

To enhance interpretability, existing studies analyzing SDOH-stroke mortality associations often adopt a preselection step on the SDOH covariates (Tsao et al. (2022, 2023)), as their number is usually large, containing hundreds of variables. Without a proper selection of SDOH covariates, direct clustering using the existing methods (Yao et al. (2011); Lu and Song (2012); Wang et al. (2023)) may be statistically inefficient due to the complex structure of longitudinal SDOH data, which confronts high-dimensional challenges and complex functional structures simultaneously. To solve this issue, one may perform variable selection in functional regression models (Wang et al. (2008); Goldsmith and Schwartz (2017); Ghosal et al. (2020); Aneiros et al. (2022); Cai et al. (2022)) prior to clustering. However, these methods typically assume that associations between covariates and responses are invariant across samples, an assumption that limits their applicability to cases with heterogeneous associations. Moreover, performing selections of SDOH prior to clustering may also introduce biases for the subsequent clustering outcome, as the selection of SDOH is unrelated to the clustering process. To overcome these challenges, it would be beneficial to connect the variable selection of functional covariates to the clustering of longitudinal associations; yet this topic is rarely discussed in the literature.

Contributions In this article, we introduce a novel method for simultaneous clustering and variable selection of longitudinal associations between Social Determinants of Health (SDOH) and stroke mortality across U.S. counties. Our approach utilizes a Finite Mixture of Functional Linear Concurrent Models (FMFLCM), incorporating a new class of penalties that pursue both smoothness and sparsity. These penalties are designed to borrow information across different clusters within the functional regression models, enhancing statistical efficiency for both clustering and variable selection while addressing collinearity among functional covariates. For estimation, we develop a novel Regularized Expectation-Maximization (REM) algorithm that integrates the proposed penalties.

This method facilitates the clustering of longitudinal associations while embedding a variable selection step for functional covariates. As a result, we can iteratively update the cluster memberships and the selected covariates within the REM algorithm, mitigating biases that may arise from selected covariates during the clustering process. Through this methodology, we provide a new data-driven approach for county-level regional division, aiming to deliver insights into region-specific stroke prevention measures for the U.S. counties.

Organization The remainder of this article is organized as follows: In Section 2 we introduce the SDOH and stroke mortality dataset and then proceed to describe some of their data features in Section 2.1. Subsequently, we present the Finite Mixture of Functional Linear Concurrent Models (FMFLCM) in Section 2.2, followed by a demonstration of the sparsity- and smoothness-pursued penalties in Section 2.3, as well as the Regularized Expectation-Maximization (REM) algorithm in Section 2.4. In Section 3 we conduct simulation studies to compare the proposed methods with competing approaches in terms of clustering performance, variable selection, and parameter estimation. In Section 4 we apply the proposed clustering method to our dataset and present the clustering results, alongside the variable selection for the SDOH covariates. We conclude with a discussion in Section 5. The codes and datasets are publicly available at <https://github.com/fl81224/Functional-Clustering-of-Longitudinal-Associations>.

2 Methodologies

2.1 Data Source

In 2020, the Agency for Healthcare Research and Quality (AHRQ) released a SDOH database to enhance understanding of community-level factors, healthcare quality and delivery, and individual health. The SDOH database contains yearly records of 345 SDOH collected from 3226 counties from 2009 to 2018. These SDOH are classified into five domains: (1) social context, such as age, race and ethnicity, and veteran status, (2) economic context, such as income and unemployment, (3) education, (4) physical infrastructure, such as housing, food insecurity, and transportation, and (5) health care contexts, such as health insurance coverage and health care access. To study the association between

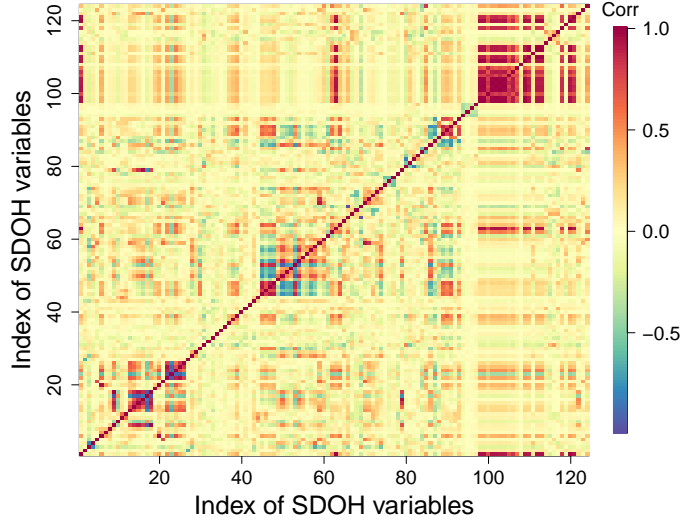


Figure 1: The correlation matrix for the SDOH variables (indexed by numbers). The correlation of the longitudinal data between the j th SDOH and j' th SDOH is calculated as $C_{j,j'}/\sqrt{C_{j,j}C_{j',j'}}$, where $C_{j,j'} = n^{-1} \sum_{i=1}^n S_i^{-1} \sum_{s=1}^{S_i} \{X_{ij}(t_{is}) - \hat{\mu}_j(t_{is})\} \{X_{ij'}(t_{is}) - \hat{\mu}_{j'}(t_{is})\}$, with $\hat{\mu}_j(\cdot)$ being the estimated mean function for the j th county. Here, $X_{ij}(t_{is})$ is the observed data of the j th SDOH at the i th county on year t_{is} , for $i = 1, \dots, n$, $j = 1, \dots, p$, and $s = 1, \dots, S_i$. The definition of $X_{ij}(t_{is})$, n , p , and S_i can be found in Section 2.2.

SDOH and stroke mortality, we connect the SDOH database with a stroke mortality data provided by the Interactive Atlas of Heart Disease and Stroke at the CDC on the county level. The stroke mortality database was originally compiled from two data sources: (1) the National Vital Statistics System at the National Center for Health Statistics and (2) the hospital discharge data from the Centers for Medicare & Medicaid Services' Medicare Provider Analysis and Review (MEDPAR) file. All data and materials used in this analysis are publicly available at the AHRQ website: <https://www.ahrq.gov/sdoh/index.html> and CDC website <https://www.cdc.gov/dhdsp/maps/atlas/index.htm>. Since the AHRQ database is HIPAA (Health Insurance Portability and Accountability Act) compliant, our data do not require to be reviewed by an institutional review board.

It is worth noting that the SDOH dataset contains missing values. Following the approach of a previous study on the dataset (Son et al. (2023)), we exclude the SDOH variables that have a missing proportion of more than 60%. The average missing proportion of the remaining variables is 3.6%. For these missing values, we employ a K-Nearest Neighbors (KNN) method (Kowarik and Templ (2016)) to impute the SDOH data, ensuring that the SDOH and stroke mortality data are aligned in time for each county.

The detailed implementation of the KNN is provided in Part A of the Supplementary Material.

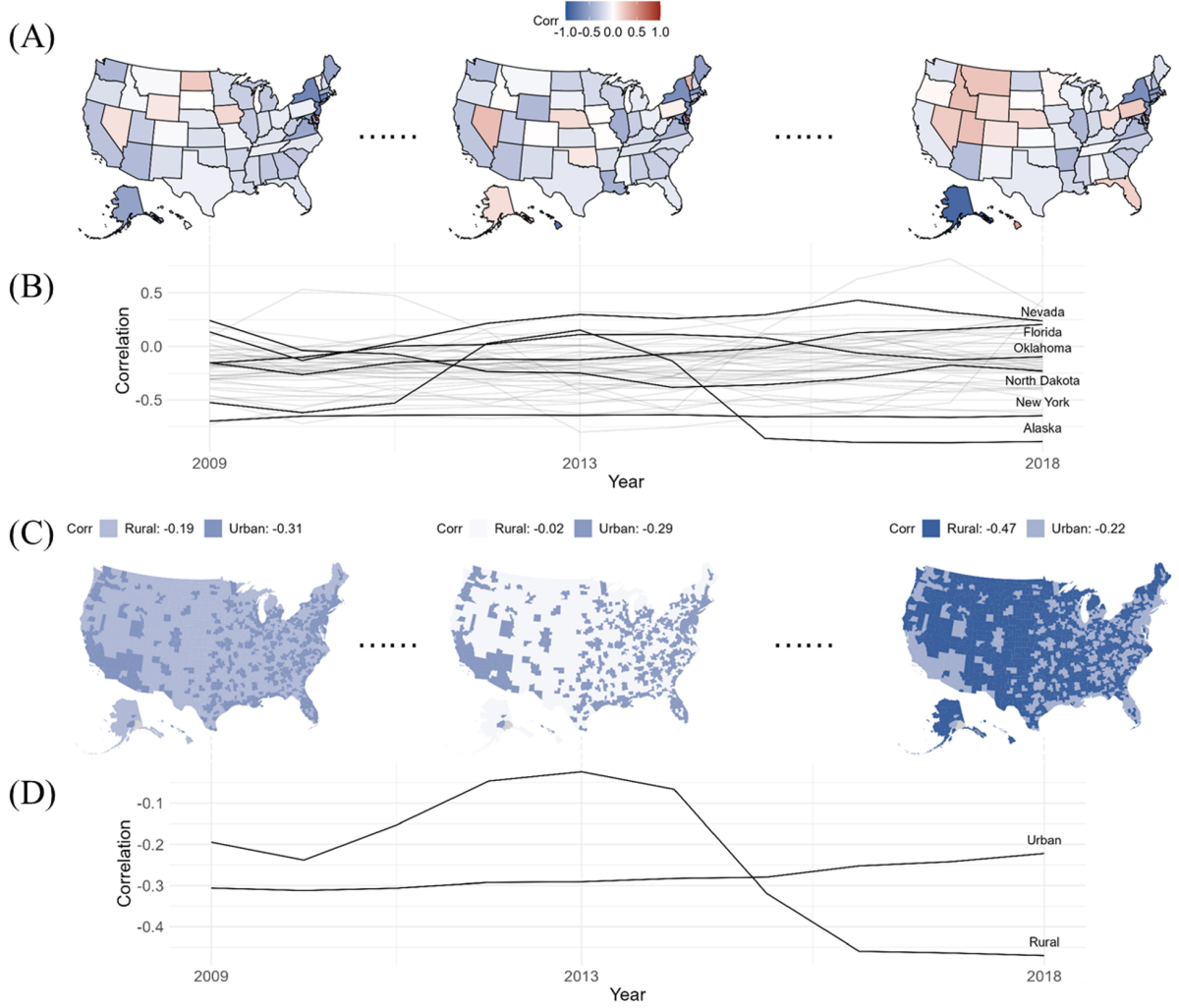


Figure 2: Statewise and rural-urban Pearson correlations between the stroke mortality and PAPL. Panels (A) and (C) are the geographical maps of correlations for the years 2009, 2013, and 2018, respectively, for two types of division strategies. Panels (B) and (D) are the statewise and rural-urban longitudinal correlations from 2009–2018, respectively.

As mentioned in the Introduction, significant collinearity may exist among the SDOH data. This phenomenon is observed in our dataset, where the longitudinal data between some of the SDOH exhibit significant correlations, as illustrated in Figure 1. Besides, coinciding with the previous studies ([Villablanca et al. \(2016\)](#); [He et al. \(2021\)](#); [Son et al. \(2023\)](#)), evident regional disparities and longitudinal variations can also be observed in the SDOH-stroke mortality associations from our dataset. To demonstrate this, we calculate the yearly Pearson correlation between stroke mortality and the percentage of Asian and Pacific Island language speakers (PAPL), an important sociocultural factor in the SDOH dataset. To calculate the yearly correlations, we adopt difference strategies to

divide counties in the U.S. into several regions, followed by calculating the correlations in each divided region. Specifically, we illustrate the correlations based on two types of divisions: statewise division (Zelko et al. (2023)) and rural-urban division (Son et al. (2023)). The yearly correlations from 2009–2018 for each state, or for rural and urban areas, are presented in panels (B) and (D) of Figure 2, respectively. Besides, we also present the geographical maps of correlations for the years 2009, 2013, and 2018 in panels (A) and (C) of Figure 2, respectively, for two types of division strategies.

From the maps in Figure 2, we observe significant regional disparities in the correlations among different states as well as between rural and urban areas. These correlations all exhibit changes over time. In addition, we find that the longitudinal correlations in rural and urban areas are quite different from the correlations from the states, as displayed in panels (B) and (D) of Figure 2. These results suggest that the outcomes of longitudinal associations are sensitive to the region division strategy, and different region divisions may lead to inconsistent conclusions for the stroke management. To address this issue, we require a reasonable data-driven method for the region division in exploring SDOH-stroke mortality associations.

2.2 Finite Mixture of Functional Linear Concurrent Models

For $i = 1, \dots, n$ and $t \in \mathcal{T}$, let $Y_i(t) \in \mathbb{R}$ and $\mathbf{X}_i(t) := (X_{i1}(t), \dots, X_{ip}(t))^\top \in \mathbb{R}^p$ represent the stroke mortality and SDOH data in the i th county at time t , respectively, where n is the number of counties and \mathcal{T} is the observed time period. Here $Y_i(\cdot)$ and $\mathbf{X}_i(\cdot)$ are considered the functional response and functional covariate for the i th subject, respectively, with n and p being the sample size and dimension of the covariates. Without loss of generality, we assume that $\mathcal{T} = [0, 1]$ in this article.

We focus on the relation between $Y_i(t)$ and $\mathbf{X}_i(t)$ for all $t \in [0, 1]$, referred to as longitudinal associations in what follows. To cluster the longitudinal associations of different counties, we assume the samples $\{Y_i(\cdot), \mathbf{X}_i(\cdot); i = 1, \dots, n\}$ can be divided into K clusters, following a finite mixture of functional linear concurrent models (FMFLCM):

$$Y_i(t) = \sum_{j=1}^p X_{ij}(t) \beta_{jk}(t) + \varepsilon_{ik}(t), \quad t \in [0, 1] \text{ if } Z_i = k, \quad (1)$$

where Z_i is the cluster membership for the i th subject, $\beta_{jk}(\cdot)$ is the functional coefficient

for the k th group reflecting the longitudinal association, and $\{\{\varepsilon_{ik}(t); t \in [0, 1]\}; i = 1, \dots, n, k = 1, \dots, K\}$ are mean-zero Gaussian processes on $[0, 1]$ that are independent across different i and k . We assume that Z_1, \dots, Z_n are independent and identically distributed (i.i.d.) samples from a multinomial distribution on $1, \dots, K$ with $\mathbb{P}(Z_i = k) = \pi_k$ and $\text{var}(\varepsilon_{ik}(t)) = \sigma_k^2$, $i = 1, \dots, n$ and $t \in [0, 1]$, where the error process $\{\varepsilon_{ik}(t); t \in [0, 1]\}$ may possess temporal correlations among different time t . By taking a fixed time $t \in \mathcal{T}$ for the functional objects in (1), this model is essentially a finite mixture of linear regression models (Peel and MacLahlan (2000); Khalili and Chen (2007); Khalili and Lin (2013)), capturing heterogeneity in the associations between $\{Y_i(t); i = 1, \dots, n\}$ and $\{(X_{i1}(t), \dots, X_{ip}(t))^\top; i = 1, \dots, n\}$ for each t . We generalize the mixture of linear regression models to its functional version in (1), aiming to account for the heterogeneity and smoothness of $\beta_{jk}(\cdot)$ during model estimation.

In the following, let $\boldsymbol{\beta}(t) = \{\beta_{jk}(t); j = 1, \dots, p; k = 1, \dots, K\}$, $\boldsymbol{\sigma}^2 := (\sigma_1^2, \dots, \sigma_K^2)^\top$, and $\boldsymbol{\pi} := (\pi_1, \dots, \pi_K)^\top$. We use $\boldsymbol{\beta}_{\cdot k}(t)$ and $\boldsymbol{\beta}_{j\cdot}(t)$ to denote the k th column and the j th row of $\boldsymbol{\beta}(t)$, respectively. For ease of notation, we might use $\boldsymbol{\beta}$, $\boldsymbol{\beta}_{\cdot k}$, $\boldsymbol{\beta}_{j\cdot}$, and β_{jk} to represent $\boldsymbol{\beta}(\cdot)$, $\boldsymbol{\beta}_{\cdot k}(\cdot)$, $\boldsymbol{\beta}_{j\cdot}(\cdot)$, and $\beta_{jk}(\cdot)$, respectively.

We assume the functional variables $Y_i(\cdot)$ and $\mathbf{X}_i(\cdot)$ in FMFLCM (1) are only observed on a finite time grid, denoted by $\{(Y_i(t_{is}), \mathbf{X}_i(t_{is})); i = 1, \dots, n, s = 1, \dots, S_i\}$, where S_i is the observed number of time points for subject i , and $\{t_{is}; i = 1, \dots, n, s = 1, \dots, S_i\}$ are time points contained in $[0, 1]$ that can be varying across different subjects. Based on the above notations, we estimate the parameters $\boldsymbol{\Phi} := (\boldsymbol{\beta}, \boldsymbol{\sigma}^2, \boldsymbol{\pi})$ by maximizing the composite log-likelihood of the data (Varin et al. (2011))

$$l(\boldsymbol{\Phi}) = \sum_{i=1}^n \sum_{s=1}^{S_i} \log \left\{ \sum_{k=1}^K \pi_k f(Y_i(t_{is}); \mathbf{X}_i(t_{is})^\top \boldsymbol{\beta}_{\cdot k}(t_{is}), \sigma_k^2) \right\}, \quad (2)$$

where $f(\cdot; \mu, \sigma^2)$ is a Gaussian density function with mean μ and variance σ^2 . In the composite likelihood, we do not consider the temporal dependencies within residual processes $\varepsilon_{ik}(\cdot)$ in order to reduce computational costs required for model estimation; similar strategies have been adopted in the estimation of functional regressions (Huang et al. (2002); Zhu et al. (2012)).

In general, optimizing $\boldsymbol{\beta}$ in (2) is an ill-posed problem due to the infinite-dimensional nature of $\boldsymbol{\beta}$. Furthermore, estimating $\boldsymbol{\beta}$ may suffer from the curse of dimensionality when p is relatively large. In such cases the estimated functional coefficients can be far from

their true values or may not even exist (Wang et al. (2008); Yi and Caramanis (2015)). To address these issues, we introduce a class of penalties in Section 2.3 to regularize the smoothness and sparsity of β simultaneously. Based on these penalties, we develop a regularized expectation maximization algorithm in Section 2.4 to simultaneously perform clustering of subjects, estimation of β , and variable selection of the covariates.

2.3 Sparsity and Smoothness Pursued Penalties

In this subsection we propose a class of smoothly clipped absolute deviation (SCAD) type penalties (Fan and Li (2001)) to adjust the aforementioned ill-posed problems. The SCAD penalty takes the form

$$\mathbf{P}_{\text{SCAD}}(u; \lambda) = \begin{cases} \lambda u & \text{if } 0 \leq u \leq \lambda, \\ -\frac{u^2 - 2\gamma\lambda u + \lambda^2}{2(\gamma-1)} & \text{if } \lambda < u < \gamma\lambda, \\ \frac{(\gamma+1)\lambda^2}{2} & \text{if } u \geq \gamma\lambda, \end{cases}$$

where u is a scalar parameter to be penalized, λ is a tuning parameter, and γ is a hyperparameter chosen to be 3.7, as suggested in Fan and Li (2001). The SCAD penalty has been shown to possess desirable theoretical properties for variable selection in various regression models (Fan and Li (2001); Wang et al. (2007, 2008)). Here we extend the penalty to the functional objects β , leading to the functional SCAD (FS) penalty

$$\mathbf{P}_{\text{FS}}(\beta; \lambda_1, \dots, \lambda_K, r) := \sum_{j=1}^p \sum_{k=1}^K \mathbf{P}_{\text{SCAD}}(\|\beta_{jk}\|_r; \lambda_k), \quad (3)$$

where $\|\beta_{jk}\|_r = \sqrt{\|\beta_{jk}\|^2 + r\|\beta_{jk}^{(2)}\|^2}$, with $\|f\| = \sqrt{\int_0^1 f^2(t) dt}$ being the L_2 norm for a function f . The norm $\|\beta_{jk}\|_r$ simultaneously measures the magnitude and smoothness of β_{jk} (Meier et al. (2009)), in which r leverages the two terms in the norm. By penalizing β using (3), we can regularize the smoothness of each β_{jk} to deal with its functional structure, and shrink the β_{jk} with small norm $\|\beta_{jk}\|_r$ to zero (Huang et al. (2009)) for the purpose of variable selection.

Recall that our SDOH functional covariates exhibit significant collinearity, as illustrated in Figure 1. This collinearity may increase variance and potentially lead to misspecification in variable selection (Zou and Hastie (2005)). To address this issue, we

adopt a similar strategy as the elastic net (Zou and Zhang (2009)) to add an L_2 term to the FS penalty (3). As such, we obtain the functional SCAD-Net (FS-Net) penalty

$$\mathbf{P}_{\text{FS-Net}}(\boldsymbol{\beta}; \lambda_1, \dots, \lambda_K, \rho, r) := \sum_{j=1}^p \sum_{k=1}^K \{ \rho \mathbf{P}_{\text{SCAD}}(\|\beta_{jk}\|_r; \lambda_k) + (1 - \rho) \lambda_k \|\beta_{jk}\|_r^2 \}, \quad (4)$$

where $\rho \in [0, 1]$ is a tuning parameter controlling the proportions between the FS penalty and the L_2 term. The above penalty not only maintains the properties of the FS penalty but also reduces variance and addresses misspecification in variable selections by penalizing the magnitude of $\sum_{j=1}^p \sum_{k=1}^K \lambda_k \|\beta_{jk}\|_r^2$.

In general, variable selection with FS or FS-Net does not guarantee that the selected covariates from different clusters are the same. This may not be suitable for some applications where identifying important variables for all clusters is necessary. In our case, the purpose of variable selection for SDOH is to aid clustering based on the selected covariates. Therefore, we require that the selected SDOH for all clusters be the same within estimation procedures. To facilitate this kind of investigation, we propose shrinking $\beta_{jk}; k = 1, \dots, K$ to zero functions simultaneously, referred to as cluster-invariant sparsity for variable selection. For this we modify the FS-Net penalty into the functional group SCAD-Net (FGS-Net) penalty

$$\mathbf{P}_{\text{FGS-Net}}(\boldsymbol{\beta}; \lambda, \rho, r) := \sum_{j=1}^p \{ \rho \mathbf{P}_{\text{SCAD}}(\|\boldsymbol{\beta}_j\|_r; \lambda) + (1 - \rho) \lambda \|\boldsymbol{\beta}_j\|_r^2 \}, \quad (5)$$

where $\|\boldsymbol{\beta}_j\|_r = \sqrt{\sum_{k=1}^K \|\beta_{jk}\|_r^2}$. By grouping $\{\beta_{kj}; k = 1, \dots, K\}$ for each j together in the norm, the FGS-Net not only yields cluster-invariant sparsity but also improves statistical efficiency for variable selection by borrowing strength across all clusters.

2.4 Regularized EM Algorithm

In this subsection we apply an EM algorithm to proceed with the parameter estimation of FMFLCM in (1). We first introduce a latent variable $z_{ik} := I(Z_i = k)$ to represent the cluster membership of the subject i , where $I(\cdot)$ is an indicator function. Denote \mathbf{Z} as $\{z_{ik}; i = 1, \dots, n, k = 1, \dots, K\}$. The composite log-likelihood of FMFLCM containing

\mathbf{Z} is then given by

$$l_C(\Phi, \mathbf{Z}) = \sum_{i=1}^n \sum_{k=1}^K z_{ik} \sum_{s=1}^{S_i} [\log \pi_k + \log \{f(Y_i(t_{is}); \{\mathbf{X}_i(t_{is})\}^\top \boldsymbol{\beta}_{\cdot k}(t_{is}), \sigma_k^2)\}]. \quad (6)$$

To address the ill-posed issue for estimating functional coefficients $\boldsymbol{\beta}$, we develop a Regularized EM (REM) algorithm by incorporating penalty functions proposed in Section 2.3. In the following we demonstrate the E-step and M-step of the REM algorithm equipped with the FGS-Net penalty (5), while those equipped with FS penalty (3) or FS-Net penalty (4) can be obtained similarly.

2.4.1 Procedures of REM algorithm

Let $\Phi^{(m-1)} := (\boldsymbol{\beta}^{(m-1)}, (\boldsymbol{\sigma}^2)^{(m-1)}, \boldsymbol{\pi}^{(m-1)})$ be the parameters updated at the $(m-1)$ th iteration. The REM algorithm iterates between the following E-step and M-step:

E-step: With the parameter $\Phi^{(m-1)}$, we first compute the conditional expectation of z_{ik} , given the samples $\mathbf{Y} = \{Y_i(t_{is}); i = 1, \dots, n, s = 1, \dots, S_i\}$ and $\mathbf{X} = \{\mathbf{X}_i(t_{is}); i = 1, \dots, n, s = 1, \dots, S_i\}$,

$$\begin{aligned} \omega_{ik}^{(m)} &:= \mathbb{E}_{\Phi^{(m-1)}}(z_{ik} | \mathbf{Y}, \mathbf{X}) \\ &= \frac{\pi_k^{(m-1)} \sum_{s=1}^{S_i} f(Y_i(t_{is}), \mathbf{X}_i(t_{is})^\top \boldsymbol{\beta}_{\cdot k}^{(m-1)}(t_{is}), (\sigma_k^2)^{(m-1)})}{\sum_{k=1}^K \pi_k^{(m-1)} \sum_{s=1}^{S_i} f(Y_i(t_{is}), \mathbf{X}_i(t_{is})^\top \boldsymbol{\beta}_{\cdot k}^{(m-1)}(t_{is}), (\sigma_k^2)^{(m-1)})}. \end{aligned} \quad (7)$$

After that, we calculate the expectation of the log-likelihood in (6) conditioning on \mathbf{Y} and \mathbf{X} , given the parameter $\Phi^{(m-1)}$. This leads to the Q function

$$Q(\Phi | \Phi^{(m-1)}) := \sum_{i=1}^n \sum_{k=1}^K \omega_{ik}^{(m)} \sum_{s=1}^{S_i} [\log \pi_k + \log \{f(Y_i(t_{is}), \{\mathbf{X}_i(t_{is})\}^\top \boldsymbol{\beta}_{\cdot k}(t_{is}), \sigma_k^2)\}]. \quad (8)$$

M-step: To facilitate the update of $\boldsymbol{\beta}$, we incorporate the FGS-Net penalty (5) into the Q function (8),

$$Q^{\text{pen}}(\Phi | \Phi^{(m-1)}; \lambda, \rho, r) := Q(\Phi | \Phi^{(m-1)}) - P_{\text{FGS-Net}}(\boldsymbol{\beta}; \lambda, \rho, r). \quad (9)$$

According to (9), we separately update the parameters $\boldsymbol{\beta}$, $\boldsymbol{\sigma}^2$, and $\boldsymbol{\pi}$, given the current tuning parameters λ, ρ, r . In detail, holding $\boldsymbol{\sigma}^2$ and $\boldsymbol{\pi}$ fixed at their previous values at

the $(m - 1)$ th iteration, we update β as

$$\beta^{(m)} = \operatorname{argmax}_{\beta} Q^{\text{pen}}((\beta, (\sigma^2)^{(m-1)}, \pi^{(m-1)}) | \Phi^{(m-1)}; \lambda, \rho, r). \quad (10)$$

Once obtaining $\beta^{(m)}$, we update $\pi^{(m)}$ by

$$\pi_k^{(m)} = \frac{\sum_{n=1}^N \omega_{ik}^{(m)}}{N}, \quad k = 1, \dots, K \quad (11)$$

and update $(\sigma^2)^{(m)}$ by

$$(\sigma_k^2)^{(m)} = \frac{\sum_{i=1}^N \omega_{ik}^{(m)} \sum_{s=1}^{S_i} \{Y_i(t_{is}) - \mathbf{X}_i(t_{is})^\top \beta_k^{(m)}(t_{is})\}^2}{\sum_{i=1}^N S_i \omega_{ik}^{(m)}}, \quad k = 1, \dots, K, \quad (12)$$

where $\omega_{ik}^{(m)}$ is defined in (7). Given (10), (11), and (12), we subsequently update $\Phi^{(m)} = (\beta^{(m)}, (\sigma^2)^{(m)}, \pi^{(m)})$ until the convergence. The stopping criteria of the REM algorithm are provided in Section B of the Supplementary Material.

Note that the main efforts for the above procedures lie in the optimization in (10). We demonstrate this process in detail in Sections 2.4.2.

2.4.2 Optimization of FGS-Net Regularization

Since we penalize the smoothness of β in (5) via controlling their second-order derivatives, we adopt a similar strategy of smoothing spline (Perperoglou et al. (2019)) to represent the functional coefficients. Specifically, we parameterize $\beta_{jk}(t)$ by the cubic spline basis functions $\psi_1(t), \dots, \psi_L(t)$, with the knots of spline functions given as $\bigcup_{i=1}^n \{t_{is}; s = 1, \dots, S_i\}$. As such, $\beta_{jk}(t)$ is represented by

$$\beta_{jk}(t) = \mathbf{b}_{jk}^\top \Psi(t), \quad t \in [0, 1], \quad (13)$$

where $\mathbf{b}_{jk} = (b_{jk1}, \dots, b_{jkL})^\top \in \mathbb{R}^L$ and $\Psi(t) = (\psi_1(t), \dots, \psi_L(t))^\top \in \mathbb{R}^L$. After that, we maximize (10) by substituting (13) into the Q function (9). We use $\mathbf{D}^\top \mathbf{D}$ to denote the Cholesky decomposition of the nonnegative definite matrix

$$\int_0^1 \Psi(t) \{\Psi(t)\}^\top + r \Psi''(t) \{\Psi''(t)\}^\top dt,$$

where $\mathbf{D} \in \mathbb{R}^{L \times L}$ is an upper triangular matrix. Given this, define $\boldsymbol{\alpha}_{jk} = \mathbf{D}\mathbf{b}_{jk} \in \mathbb{R}^L$ and $\boldsymbol{\alpha}_j = (\boldsymbol{\alpha}_{j1}^\top, \dots, \boldsymbol{\alpha}_{jK}^\top)^\top \in \mathbb{R}^{LK}$. We rewrite $\|\boldsymbol{\beta}_j\|_r$ as

$$\begin{aligned}\|\boldsymbol{\beta}_j\|_r &= \sqrt{\|\boldsymbol{\beta}_j\|^2 + r\|(\boldsymbol{\beta}_j)''\|^2} \\ &= \sqrt{\sum_{k=1}^K \int_0^1 \mathbf{b}_{jk}^\top \boldsymbol{\Psi}(t) \{\boldsymbol{\Psi}(t)\}^\top \mathbf{b}_{jk} + r \mathbf{b}_{jk}^\top \boldsymbol{\Psi}''(t) \{\boldsymbol{\Psi}''(t)\}^\top \mathbf{b}_{jk} dt} \\ &= \sqrt{\sum_{k=1}^K (\mathbf{D}\mathbf{b}_{jk})^\top \mathbf{D}\mathbf{b}_{jk}} = \|\boldsymbol{\alpha}_j\|,\end{aligned}$$

where we abuse the notation $\|\cdot\|$ to denote the Euclidean norm of a vector. We further denote $\boldsymbol{\alpha} = (\boldsymbol{\alpha}_1^\top, \dots, \boldsymbol{\alpha}_p^\top)^\top \in \mathbb{R}^{pLK}$ and $\mathbf{h}_{ij}(t) = X_{ij}(t) \cdot ((\psi_1(t), \dots, \psi_L(t))\mathbf{D}^{-1})^\top \in \mathbb{R}^L$. With these notations we can transform the optimization (10) into a standard group SCAD- L_2 optimization problem (Zeng and Xie (2014)) as follows:

$$\operatorname{argmax}_{\boldsymbol{\alpha}} \left[L_m(\boldsymbol{\alpha}) - \sum_{j=1}^p \left\{ \rho \mathbf{P}_{\text{SCAD}}(\|\boldsymbol{\alpha}_j\|; \lambda) + (1 - \rho)\lambda \|\boldsymbol{\alpha}_j\|^2 \right\} \right], \quad (14)$$

where

$$L_m(\boldsymbol{\alpha}) = \sum_{i=1}^n \sum_{k=1}^K \omega_{ik}^{(m)} \sum_{s=1}^{S_i} \left[\log \pi_k^{(m-1)} + \log \left\{ f \left(Y_i(t_{is}), \sum_{j=1}^p \mathbf{h}_{ij}^\top(t_{is}) \boldsymbol{\alpha}_{jk}, (\sigma_k^2)^{(m-1)} \right) \right\} \right].$$

The above optimization can be efficiently solved by the group coordinate descent algorithm (Breheny and Huang (2015)). Once we obtain the maximizer of $\boldsymbol{\alpha}_{jk}$ from (14), denoted by $\boldsymbol{\alpha}_{jk}^{(m)}$, we can estimate the (j, k) th element of $\boldsymbol{\beta}^{(m)}$ by

$$\beta_{jk}^{(m)}(t) = (\mathbf{D}^{-1} \boldsymbol{\alpha}_{jk}^{(m)})^\top \boldsymbol{\Psi}(t), \quad t \in [0, 1]. \quad (15)$$

For each j , the penalty in (14) encourages $\boldsymbol{\alpha}_{jk}^{(m)}$, $k = 1, \dots, K$, to be zero vectors simultaneously. The functional coefficients $\{\beta_{jk}^{(m)}; k = 1, \dots, K\}$ are smooth functions, and they become zero functions simultaneously as λ increases, satisfying the cluster-invariant sparsity.

We similarly establish the REM algorithms for the FS penalty (3) or FS-Net penalty

(4) by modifying the penalty function in (14) as

$$\begin{aligned} \text{FS: } & \sum_{k=1}^K \sum_{j=1}^p \mathbf{P}_{\text{SCAD}}(\|\boldsymbol{\alpha}_{jk}\|; \lambda_k), \\ \text{FS-Net: } & \sum_{k=1}^K \sum_{j=1}^p \{\rho \mathbf{P}_{\text{SCAD}}(\|\boldsymbol{\alpha}_{jk}\|; \lambda_k) + (1 - \rho) \lambda_k \|\boldsymbol{\alpha}_{jk}\|^2\}. \end{aligned}$$

In these two cases, $\{\boldsymbol{\alpha}_{jk}^{(m)}, k = 1, \dots, K\}$ are not encouraged to be zero vectors simultaneously, only obtaining the cluster-variant sparsity during estimation.

2.5 Tuning Strategies

The REM algorithm requires tuning of three hyperparameters λ , ρ , and r . The traditional strategy for choosing λ , ρ , and r needs to run the entire algorithm for all candidate combinations of (λ, ρ, r) . This is computationally inefficient since there are numerous choices of candidate combinations that need to be examined. Inspired by the path-fitting algorithm (Breheny and Huang (2015)) for a fast tuning of λ , we modify the traditional tuning strategy for our REM algorithm. Instead of running a complete REM for each candidate of λ , we propose to tune λ in each M-step of the REM algorithm; refer to Part B.1 in the Supplementary Material for the implementation details. Using this approach, we can accelerate the tuning process by employing a path-fitting algorithm to select λ , similar to the existing literature (Huang et al. (2009); Li et al. (2016); Cai et al. (2019)).

For the hyperparameters ρ and r , we run an entire REM for each of their candidate combinations, nested with the aforementioned strategy for tuning λ . Since ρ and r are imposed to penalize functional smoothness and improve prediction performance, we adopt the Akaike Information Criterion (AIC) for the selection of ρ and r , as AIC offers a predictive criterion for model selection (Ding et al. (2018)). Specifically, the AIC is calculated as

$$\text{AIC}(\rho, r) = -2l(\hat{\boldsymbol{\Phi}}(\rho, r)) + 2\text{df}(\rho, r), \quad (16)$$

where $l(\cdot)$ is defined in (2), $\hat{\boldsymbol{\Phi}}(\rho, r)$ is the converged parameters of the REM algorithm, given the current choices of ρ and r , and $\text{df}(\rho, r)$ is the degree of freedom determined by ρ and r . In addition, we select the number of clusters K using Bayesian information criterion (BIC), a widely used criterion for model-based clustering procedure (Keribin (2000); James and Sugar (2003); Ding et al. (2018); Liang et al. (2021)). The BIC is

given as

$$\text{BIC}(K) = -2l(\Phi_K) + \text{df}(K) \cdot \log\left(\sum_{i=1}^n S_i\right), \quad (17)$$

where Φ_K denotes the converged parameter $\widehat{\Phi}(\rho, r)$ with ρ and r selected by (16) and the number of clusters being K , and $\text{df}(K)$ is the degree of freedom determined by K . For the detailed definitions of $\text{df}(\rho, r)$ and $\text{df}(K)$ in AIC (16) and BIC (17), please refer to [Breheny and Huang \(2015\)](#).

3 Simulation

In this section, we conduct numerical simulations to assess the performances of the proposed method in Section 2, in comparison to other competing methods across three aspects: clustering, variable selection, and parameter estimation.

3.1 Data Generation

We generate the functional covariates $\mathbf{X}_i(\cdot)$, $i = 1, \dots, n$, by

$$\mathbf{X}_i(t) = \sum_{l=1}^4 \boldsymbol{\theta}_{il} \psi_l(t), \quad \forall t \in [0, 1],$$

where $\psi_1(\cdot), \dots, \psi_4(\cdot)$ are the first four nonconstant Fourier basis functions, and $\boldsymbol{\theta}_{il} \in \mathbb{R}^p$, for each i and l , is a random vector sampled from a mean-zero Gaussian distribution with the covariance matrix $(l^{-2}\alpha^{|j-k|})_{1 \leq j, k \leq p} \in \mathbb{R}^{p \times p}$. The parameter α controls the dependence among covariates, with a higher value indicating stronger dependencies.

To generate the functional coefficients attaining the cluster-invariant sparsity, we set $\boldsymbol{\beta}_{\cdot k}(t) \in \mathbb{R}^p$ as

$$\boldsymbol{\beta}_{\cdot k}(t) = (f_{1k}(t), f_{1k}(t), f_{2k}(t), f_{2k}(t), f_{3k}(t), f_{3k}(t), 0, \dots, 0)^\top, \quad k = 1, \dots, K, t \in [0, 1],$$

where $f_{jk}(t) = f_{jk}^*(t)/\|f_{jk}^*\|_2$, and $f_{jk}^*(\cdot)$ s are given by

$$\begin{aligned} f_{11}^*(t) &= \sin\left(\frac{\pi t}{2} + \frac{3\pi}{2}\right) - t - \frac{1}{2}, & f_{12}^*(t) &= \{\cos(2\pi t) - 1\}^2, \\ f_{13}^*(t) &= -f_{11}^*(t) + 1, & f_{21}^*(t) &= \sin(2\pi t) - t + 0.5, \\ f_{22}^*(t) &= \sin\left(\frac{\pi t}{2} + \pi\right), & f_{23}^*(t) &= -f_{21}^*(t) - 0.5, \\ f_{31}^*(t) &= -\sin\left(\frac{\pi t}{2} + \frac{3\pi}{2}\right) - t - 0.5, & f_{32}^*(t) &= -f_{12}^*(t), \\ f_{33}^*(t) &= f_{11}^*(t) + t + 0.5. \end{aligned}$$

These functions are presented in Figure 2 in the Supplementary Material. It is worth noting that the relevant covariates for all clusters are X_{i1}, \dots, X_{i6} , each of which makes an equal contribution to Y_i since $\|f_{jk}\|_2 = 1$ for $j = 1, \dots, 6$ and $k = 1, \dots, K$. We set the number of clusters $K = 3$.

Next, we generate the cluster membership Z_i from a multinomial distribution as described in Section 2, with $\pi_k = 1/K, k = 1, \dots, K$. Providing $\mathbf{X}_i(t), Z_i$, and $\boldsymbol{\beta}(t)$, $Y_i(t)$ is generated from the model (1) for each t , where the $\varepsilon_{ik}(t)$ is constructed as $\tilde{\varepsilon}_{ik}(t) + \tau_{ik}$. For each i and k , $\{\tilde{\varepsilon}_{ik}(t); t \in [0, 1]\}$ are independent mean-zero Gaussian processes with the covariance function $\sigma_k^2 \exp(-|t_1 - t_2|)/2$, and τ_{ik} s are Gaussian measurement noises with variance $\sigma_k^2/2$. The variance of the error terms σ_k^2 is taken according to the signal-to-noise ratio (SNR)

$$\sigma_k^2 = \left\{ \frac{\sum_{i=1}^n \int_0^1 \sum_{k=1}^K I(Z_i = k) \{\mathbf{X}_i(t)^\top \boldsymbol{\beta}_{\cdot k}(t)\}^2 dt}{n} \right\} / \text{SNR},$$

with SNR being set as 12. Finally, the observed time points $\{t_{is}; s = 1, \dots, S_i\}$ for functional data are set as 10 equally spaced knots on $[0, 1]$ for each i , mimicking the setting of our SDOH data.

Based on the above setting, we evaluate the method proposed in Section 2, which is denoted as FGS-Net due to the use of FGS-Net penalty (5). We compare FGS-Net by other REM methods penalized with the FS-Net penalty (4) and FS penalty (3), denoted as FS-Net and FS in what follows. Apart from these three methods, we examine the following competing methods for clustering longitudinal associations:

- RP: This method incorporates a roughness penalty (RP) into the REM algorithm,

which is given as $\sum_{j=1}^p \sum_{k=1}^K \lambda \|\beta_{jk}''\|_2^2$.

- VS-RP: This method initially employs the FGS-Net within the finite mixture of functional linear concurrent model (1), setting $K = 1$ for variable selection (VS). This method is denoted as FMFLCM(1), encompassing several existing methods (Wang et al. (2008); Goldsmith and Schwartz (2017); Ghosal et al. (2020)) as special cases. Subsequently, the preselected variables are used to implement the RP method for clustering.
- LI-MIX: This method fits the data by a finite mixture of linear regression models (LI-MIX), that is, the functional coefficient $\beta_{jk}(t)$ in (1) is treated as a constant over t . To preform this method, we first conduct a variable selection using conventional linear regression models shrunk with an elastic-net penalty (Zou and Zhang (2009)). After that, we adopt the selected covariates to fit a finite mixture of linear regression models for the clustering (Peel and MacLahlan (2000); Khalili and Chen (2007); Khalili and Lin (2013)).

The RP is a simplification of the FS-Net penalty (4) with $\rho = 0$, which only regularizes the roughness of each β_{jk} and does not yield sparsity. VS-RP and LI-MIX are two two-step approaches, which implement the variable selection and clustering orderly. These two-step methods are more simple than the aforementioned FGS-Net, FS-Net, FS, and RP. However, selecting relevant covariates prior to the clustering procedure may raise additional problems, as the clustering performance may be sensitive to the outcome from the variable selection. It is worth noting that the two-step method LI-MIX further ignores the time-varying nature of β_{jk} .

For each scenario with different combinations of n , p , and α , the simulations are repeated 100 times. We adopt random initialization for the FGS-Net, FS-Net, and FS methods by setting $\omega_{ik}^{(0)} = I(Z_i^{(0)} = k)$, where $Z_i^{(0)}$ is sampled from a multinomial distribution over $\{1, \dots, K\}$ with equal probabilities. On the other hand, RP, VS-RP, and LI-MIX are initialized with the actual cluster membership $\omega_{ik}^{(0)} = I(Z_i = k)$. To alleviate computation burdens, we only use one initialization for each simulation. Moreover, the K in RP, VS-RP, and LI-MIX is fixed to 3, the true number of clusters. The K for FGS-Net, FS-Net, and FS are selected based on (17).

The performance of clustering, variable selection, and parameter estimation is evaluated based on the following criteria:

- Clustering accuracy is evaluated using the adjusted Rand Index (ARI, [Rand \(1971\)](#)). The ARI is bounded by ± 1 to measures the similarity between the true cluster membership and the estimated cluster membership. A higher ARI represents a better clustering result.
- Variable selection performance is evaluated using C and IC, where C is the number of zero coefficients that are correctly estimated to zero $C = \sum_{j=7}^p \sum_{k=1}^K I(\|\hat{\beta}_{jk}\|_2 = 0)$, where $\hat{\beta}_{jk}$ is the estimate of β_{jk} . Similarly, IC is the number of nonzero coefficients that are incorrectly estimated to zero $IC = \sum_{j=1}^6 \sum_{k=1}^K I(\|\hat{\beta}_{jk}\|_2 = 0)$.
- The parameter estimation accuracy is measured using the standardized mean square error (MSE) of the functional coefficients: $MSE = \frac{\sum_{k=1}^K \sum_{j=1}^p \|\beta_{jk} - \hat{\beta}_{jk}\|_2^2}{\sum_{k=1}^K \sum_{j=1}^p \|\beta_{jk}\|_2^2}$.

3.2 Result

We investigate the performances of different methods under various scenarios of n , p , and α . Here we set n to 180 or 300 and take p as $10, n/6, n/2$, and $3n/4$, to consider the situations ranging from a small to a large number of covariates. Additionally, we set α to 0.4 and 0.8 to reflect the mild or strong dependence among the covariates. The averaged ARI, C, IC, and MSE are presented in Table 1. In the analysis below, we only focus on the results of $n = 180$. Similar conclusions can be obtained for the result of $n = 300$.

Overall, FGS-Net, FS-Net, and FS demonstrate superior performance across various scenarios with different values of n , p , and α , underscoring the benefits of simultaneously implementing variable selection and clustering under the REM framework. In contrast, the RP method, which only applies a roughness penalty and omits variable selection within the clustering process, quickly deteriorates in performance for both clustering and parameter estimation as p increases. Among the two-step methods, we find that VS-RP performs poorly compared to the first three REM-type methods. For instance, in all scenarios with $n = 180$, the average ICs of VS-RP are mostly larger than 9, indicating that about half of the nonzero functional coefficients are incorrectly identified as zero. These results lead to significant estimation errors in both clustering and parameter estimation by the VS-RP method, suggesting that selecting variables prior clustering is ineffective. Notably, the performance of LI-MIX is even poorer, as this method additionally ignore the time-varying nature of $\beta(\cdot)$ during the estimation process.

Table 1: Averaged ARI, C, IC, and MSE for FGS-Net, FS-Net, FS, RP, VS-RP, and LI-MIX with $p = 10, n/6, n/2, 4n/3$, $\alpha = 0.4, 0.8$, $n = 180, 300$. The highest ARI, C, and lowest IC, MSE are in bold.

$n = 180$																	
		$p=10$				$p=30$				$p=100$				$p=240$			
	Model	ARI	C	IC	MSE	ARI	C	IC	MSE	ARI	C	IC	MSE	ARI	C	IC	MSE
$\alpha = 0.4$	Truth	1	12	0	0	1	72	0	0	1	252	0	0	1	702	0	0
	RP	1.00	0.00	0.00	0.04	0.01	0.00	0.00	1.00	0.01	0.00	0.00	1.00	0.01	0.00	0.00	1.00
	VS-RP	0.49	11.94	7.59	0.60	0.46	71.61	7.56	0.61	0.37	250.86	7.50	0.65	0.30	699.00	6.90	0.70
	LI-MIX	0.28	4.89	2.58	0.72	0.22	36.30	2.82	0.81	0.07	139.11	2.85	1.24	0.01	388.71	3.09	2.76
	FS	1.00	11.99	0.00	0.02	0.99	71.99	0.12	0.02	0.94	251.80	0.97	0.13	0.87	701.73	2.18	0.24
	FS-Net	1.00	12.00	0.00	0.02	0.99	72.00	0.12	0.02	0.94	251.84	1.00	0.12	0.87	701.90	2.28	0.24
	FGS-Net	1.00	12.00	0.00	0.02	1.00	72.00	0.00	0.02	0.99	252.00	0.00	0.06	0.97	702.00	0.33	0.08
$\alpha = 0.8$	Truth	1	12	0	0	1	72	0	0	1	252	0	0	1	702	0	0
	RP	1.00	0.00	0.00	0.09	0.01	0.00	0.00	0.99	0.01	0.00	0.00	1.00	0.01	0.00	0.00	1.00
	VS-RP	0.77	11.49	10.41	0.88	0.74	70.92	10.50	0.89	0.73	250.44	10.20	0.87	0.66	699.24	10.62	0.90
	LI-MIX	0.23	6.06	3.96	0.88	0.19	43.44	4.32	1.00	0.08	145.47	4.47	1.98	0.01	426.78	5.10	4.93
	FS	0.99	11.91	1.86	0.21	0.99	70.62	2.23	0.25	0.99	249.03	3.39	0.34	0.96	701.88	8.51	0.77
	FS-Net	0.99	11.90	0.53	0.11	0.99	71.04	0.61	0.12	0.99	249.55	1.23	0.16	0.97	701.87	6.71	0.55
	FGS-Net	1.00	12.00	0.15	0.09	0.99	72.00	0.27	0.11	0.99	252.00	0.36	0.13	0.98	701.97	1.08	0.17
$n = 300$																	
		$p=10$				$p=50$				$p=150$				$p=400$			
	Model	ARI	C	IC	MSE	ARI	C	IC	MSE	ARI	C	IC	MSE	ARI	C	IC	MSE
$\alpha = 0.4$	Truth	1	12	0	0	1	132	0	0	1	432	0	0	1	1182	0	0
	RP	1.00	0.00	0.00	0.04	0.01	0.00	0.00	1.00	0.01	0.00	0.00	1.00	0.00	0.00	0.00	1.00
	VS-RP	0.88	11.82	3.33	0.25	0.87	131.22	3.42	0.25	0.88	430.11	3.54	0.26	0.85	1177.29	3.42	0.28
	LI-MIX	0.31	4.77	1.26	1.14	0.25	65.34	1.65	1.19	0.09	232.98	1.59	1.42	0.01	632.7	1.59	2.99
	FS	1.00	12.00	0.00	0.01	0.99	131.99	0.08	0.03	0.99	431.98	0.06	0.03	0.99	1181.93	0.15	0.03
	FS-Net	1.00	12.00	0.00	0.01	0.99	132.00	0.10	0.03	0.99	432.00	0.07	0.03	0.99	1181.97	0.16	0.03
	FGS-Net	1.00	12.00	0.00	0.01	1.00	132.00	0.00	0.01	1.00	432.00	0.00	0.01	0.99	1182.00	0.00	0.02
$\alpha = 0.8$	Truth	1	12	0	0	1	132	0	0	1	432	0	0	1	1182	0	0
	RP	1.00	0.00	0.00	0.07	0.01	0.00	0.00	0.99	0.01	0.00	0.00	1.00	0.01	0.00	0.00	1.00
	VS-RP	0.92	11.73	8.04	0.7	0.91	130.92	7.89	0.7	0.9	429.57	7.74	0.68	0.85	1175.85	8.13	0.69
	LI-MIX	0.24	6.42	2.88	1.16	0.2	80.13	2.91	1.26	0.08	263.16	3.3	1.82	0.02	747.66	3.57	4.57
	FS	1.00	12.00	0.00	0.04	1.00	131.65	0.00	0.08	0.99	430.79	0.09	0.04	0.97	1181.97	8.02	0.72
	FS-Net	1.00	11.99	0.00	0.04	1.00	131.74	0.00	0.04	0.99	431.05	0.07	0.04	0.98	1181.96	6.14	0.49
	FGS-Net	0.99	12.00	0.00	0.04	0.99	132.00	0.06	0.04	1.00	432.00	0.00	0.04	0.99	1182.00	0.30	0.09

In Table 1 we observe that the ICs and MSEs of FS are significantly larger than those of FS-Net as α increases. This is expected since the dependencies between functional covariates may impede the performance of the FS procedure. Incorporating an additional ridge-type penalty in FS-Net could help stabilize the estimation process for both variable selection and parameter estimation. Moreover, as p increases, the ICs and MSEs of FS-Net become further larger than those of FGS-Net. In these scenarios, the high dimensionality may undermine the statistical efficiency for both variable selection and clustering in FS-Net. Therefore, it would be beneficial to impose cluster-invariant sparsity through FGS-net to borrow strength across all clusters during estimation.

In the case of $n = 180$, $p = 240$, and $\alpha = 0.8$, we further illustrate the estimation performance of the functional coefficients in Figure 3. We observe that the estimations of FS-Net exhibit smaller biases, compared to FS, highlighting the significance of FS-Net in mitigating biases of functional coefficients. In comparison to the results of FS-Net and FS, the estimated curves of FGS-Net show even smaller biases and narrower confidence

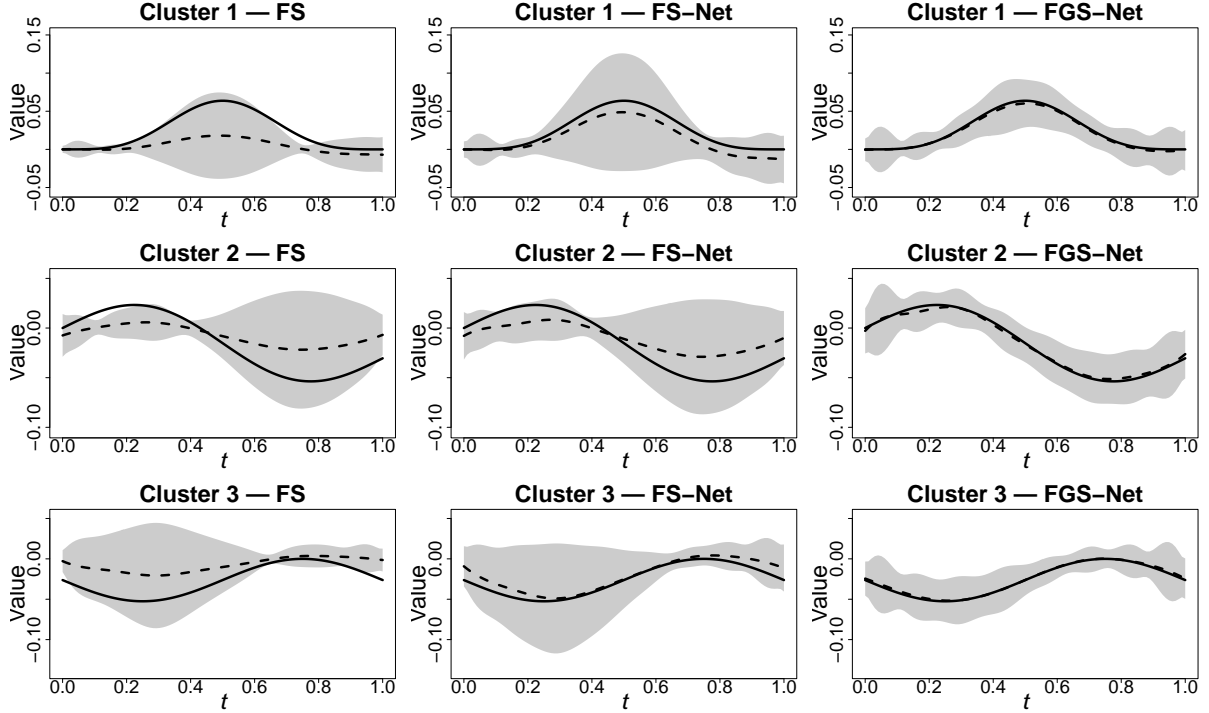


Figure 3: The true curves of the functional coefficients β_{jk} from each cluster k and their estimations from FS, FS-Net, and FGS-Net, for $n = 180$, $p = 240$, and $\alpha = 0.8$. The solid black lines represents the true curve, while the dashed lines, along with their corresponding bands, represent the pointwise means and the 95% confidence bands over 100 replicated simulations.

bands, owing to the pursuit of cluster-invariant sparsity.

In Section C.4 of the Supplementary Material, we assess the computational cost of FGS-Net in comparison to the two-step methods VS-RP and LI-MIX. Our findings indicate that, while the two-step methods are computationally faster than those utilizing REM algorithms, their performance is generally inferior, as shown in Table 3, due to the uncorrelatedness of the variable selection and clustering steps. Additionally, we observe that the computational cost of FGS-Net does not increase too rapidly as n and p increase. This suggests tolerable computational costs for simultaneously clustering and variable selection in longitudinal associations for large datasets.

4 Real data

In this section we apply our methods to the SDOH and stroke mortality dataset for clustering their longitudinal associations. Given that the stroke mortality data are right-skewed and take positive values, we conduct a log transformation to stabilize its variance. Besides, we normalize the data $X_{ij}(t_{S_i})$ by $(\sum_i S_i)^{-1} \sum_{i=1}^n \sum_{s=1}^{S_i} X_{ij}(t_{S_i})^2$ to ensure that

the SDOH covariates are on the same scale.

Performance Comparison We apply the proposed FS-Net and FGS-Net to the dataset and compare these methods with FMFLCM(1) (Wang et al. (2008); Goldsmith and Schwartz (2017); Ghosal et al. (2020)) and the LI-MIX method (Peel and MacLahlan (2000); Khalili and Chen (2007); Khalili and Lin (2013)) in the simulation section. Notably, FMFLCM(1) is a special case of the FMFLCM in (1) with $K = 1$, indicating that it does not cluster longitudinal associations during variable selection. Furthermore, LI-MIX does not account for longitudinal changes in the SDOH-stroke mortality associations during clustering, and FS-Net focuses only on cluster-variant sparsity in model estimation. Detailed comparisons of these methods are presented in Section C.3 of the Supplementary Material. Overall, FMFLCM(1) and LI-MIX tend to select a large number of covariates but fail to adequately fit the data. In contrast, FS-Net and FGS-Net provide a more accurate fit, highlighting the importance of accommodating longitudinal changes and heterogeneity when analyzing associations between SDOH and stroke mortality.

It is worth noting that the model in FS-Net has a higher complexity, compared to that of FGS-Net, with the latter pursuing cluster-invariant sparsity rather than cluster-variant sparsity. In our analysis we find that both methods achieved the fitting residuals of 0.15, and their performances are quite similar in terms of clustering and variable selection. These findings suggest that the increased complexity of FS-Net does not result in significant improvements in model fitting. For a more interpretable result, we focus only on the data analysis of FGS-Net in the remaining and refer to Section C.3 of the Supplementary Material for the results of FS-Net.

Data Analysis Using FGS-Net, we identify two clusters for the longitudinal associations and 18 relevant SDOH covariates for stroke mortality. The two clusters for the county-level longitudinal associations are presented in Figure 4. The proportions of two clusters, determined by the number of counties, stand at 68% and 32%, respectively. Notably, both clusters are prevalent across the majority of states in the U.S., encompassing both rural and urban areas (urban: 76% and 24%, and rural: 65% and 35%, for cluster 1 and cluster 2, respectively). It is worth noting that the southeastern U.S. contains a region called the Stroke Belt (Heyden et al. (1978); Lanska and Kuller (1995); Karp

et al. (2016); Howard and Howard (2020)), known for its persistent high relative excess of stroke mortality. Despite counties in the Stroke Belt having similar stroke severity, this area is also mixed by the two clusters, with proportions of 70% and 30%, respectively. These results suggest that regions sharing similar geographic and stroke characteristics may have very different SDOH-stroke mortality associations, and we may need to consider separating two types of policies for the SDOH adjustments in stroke management based on our clustering results.

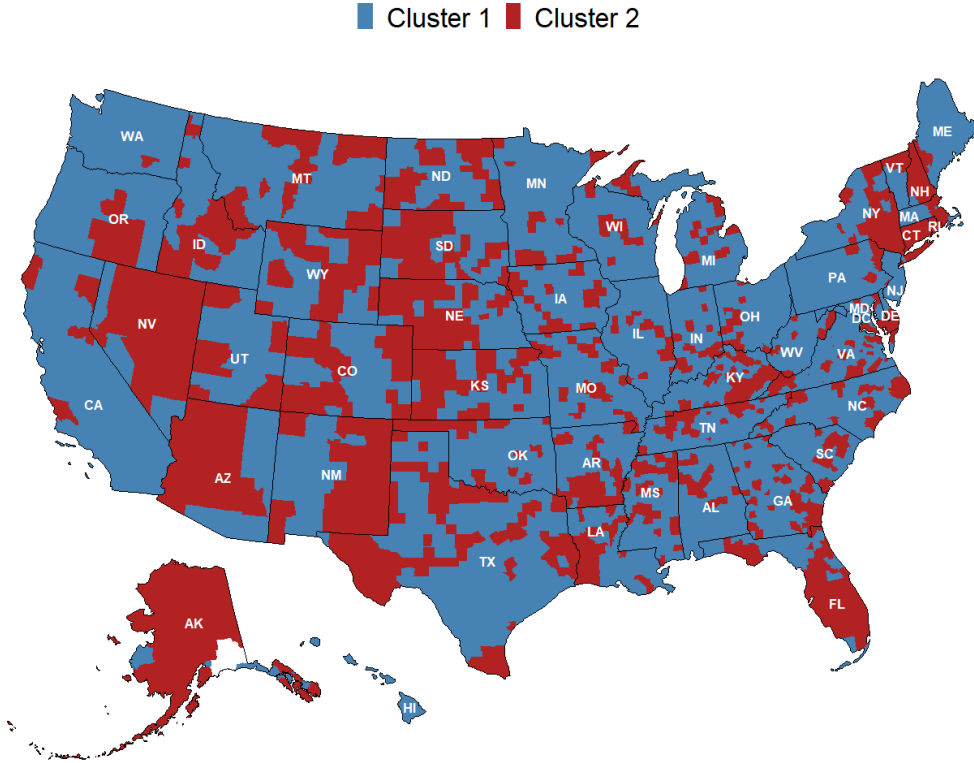


Figure 4: The clustering result for the county-level longitudinal associations between the SDOH and stroke mortality in the US.

In addition, we illustrate the selected 18 covariates of SDOH in Table 2, ordered by their relative importance (Grömping (2007)), defined as

$$\text{RI}(\beta_{j\cdot}) = \|\beta_{j\cdot}\|_2 \left\{ \frac{1}{n} \sum_{i=1}^n \left\| X_{ij} - \frac{1}{n} \sum_{i=1}^n X_{ij} \right\|^2 \right\}^{1/2}.$$

We find that the influence of the SDOH on stroke mortality is mainly contributed by four aspects: social environment, built environment, health care system, and biology. Beyond the well-studied determinants from economic, cultural, and racial domains (Tsao et al. (2023)), we find that stroke mortality is significantly associated with living and work-

ing environments, education level, and overuse of opioids. Typically, among the selected variables of SDOH, most of them are related to economic development. For example, in Table 2, MEDIAN_HOME_VALUE may reflect overall economic development and infrastructure building in the community. Additionally, a higher value of ELDERLY_RENTER may suggest a larger elderly population with lower income, facing issues such as housing instability. These economic-related factors may be potentially adjusted through more equitable economic policies. For example, MEDIAN_HOME_VALUE can be adjusted by facilitating economic development. In addition, serving as a sign of the elderly living condition, ELDERLY_RENTER can be adjusted by improving elderly welfare.

Table 2: The selected SDOH variables ranked by descent order of their relative importance.

Variable	Explanation	SDOH Domain
MEDIAN_HOME_VALUE	Median home value of owner-occupied housing units	Sociocultural Environment
NO_ENGLISH	Population that does not speak English at all, %	Sociocultural Environment
ASIAN_LANG	Population that speaks Asian and Pacific Island languages, %	Sociocultural Environment
ELDERLY_RENTER	Rental units occupied by householders aged 65 and older, %	Built Environment
GINI_INDEX	Gini index of income inequality	Sociocultural Environment
HOME_WITH_KIDS	Owner-occupied housing units with children, %	Built Environment
AGRI_JOB	Employed working in agriculture, forestry, fishing and hunting, and mining, %	Sociocultural Environment
NO_VEHICLE	Housing units with no vehicle available, %	Built Environment
OPIOID	Number of opioid prescriptions per 100 persons	Health Care System
WEAK_ENGLISH	Population that does not speak English well, %	Sociocultural Environment
BLACK	Population reporting Black race, %	Biology
BACHELOR	Population with a bachelor’s degree, %	Sociocultural Environment
NO_FUEL_HOME	Occupied housing units without fuel, %	Built Environment
TIME	Time Effect	Sociocultural Environment
ONLY_ENGLISH	Population that only speaks English, %	Sociocultural Environment
MOBILE_HOME	Housing units that are mobile homes, %	Built Environment
BELOW_HIGH_SCH	Population with less than high school education, %	Sociocultural Environment
DRIVE_2WORK	Workers taking a car, truck, or van to work, %	Built Environment

To further quantify the longitudinal associations between SDOH and stroke mortality, we investigate the functional coefficients β_{jk} estimated from the dataset. Here we only focus on the coefficients from the leading four important SDOH, which are MEDIAN_HOME_VALUE, NO_ENGLISH, ASIAN_LANG, and ELDERLY_RENTER. The longitudinal associations in the two clusters, along with the 95% confidence bands, are

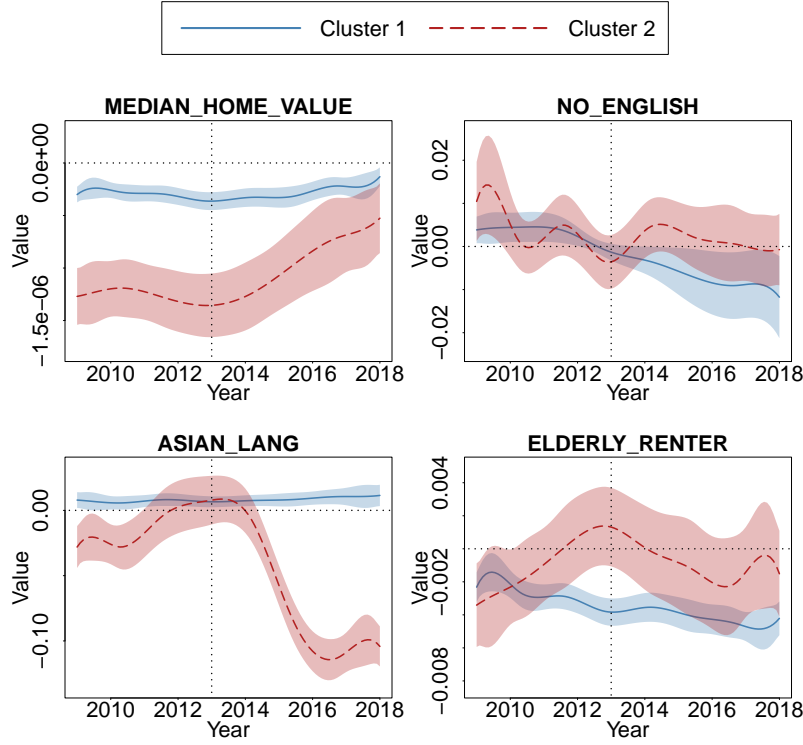


Figure 5: The estimated longitudinal associations for the leading four SDOH in two clusters. The dotted horizontal line in each sub-figure represents the zero line for the SDOH-stroke mortality longitudinal associations, and the dotted vertical line in each sub-figure indicates the common reflection point of the longitudinal associations in cluster 2.

shown in Figure 5. These 95% confidence bands are constructed using a wild-bootstrap procedure similar to those in [Zhu et al. \(2012\)](#). The detailed bootstrap procedure and its effectiveness are demonstrated in Section C.2 of the Supplementary Material.

In Figure 5 we observe that the leading four SDOH possess time-varying associations with stroke mortality. Furthermore, these associations are notably different between the two clusters. For example, the fluctuation of the longitudinal associations in cluster 2 is more significant than those in cluster 1. Additionally, we observe that, in cluster 2, all four associations exhibit a common inflection point in 2013 (the dotted vertical lines in Figure 5). These findings help us better understand the dynamics of the associations between SDOH and stroke mortality in the U.S..

In Figure 5, MEDIAN_HOME_VALUE shows a stable and weak association with stroke mortality for the counties in cluster 1, while those in cluster 2 exhibit a more intense negative effect with stroke mortality. The situation for ELDERLY_RENTER differs with the association in cluster 2 showing significant fluctuation, while that in cluster 1 presents a time-increasing negative association with stroke mortality.

As economic-related factors, MEDIAN_HOME_VALUE and ELDERLY_RENTER have been identified to significantly associate with stroke mortality ([Rodgers et al. \(2019\)](#); [Mawhorter et al. \(2023\)](#)). Our findings not only align with existing literature but also provide further insights into more tailored stroke mortality prevention strategies related to SDOH variables. For instance, the notable negative association between MEDIAN_HOME_VALUE and stroke mortality in cluster 2 highlights the importance of focusing on infrastructure development, maintenance, and enhancing overall economic equity in these regions. Noting the time-increasing negative association between ELDERLY_RENTER and stroke mortality in cluster 1, it may be beneficial to prioritize viable housing programs for lower-income elderly populations in these regions.

In addition, NO_ENGLISH and ASIAN_LANG are SDOH variables that measure the sociocultural environment of the county. NO_ENGLISH, which indicates the percentage of the population that does not speak English, is associated with stroke mortality in both clusters, with the direction of the associations shifting from positive to negative. A similar decreasing trend is observed in the association between ASIAN_LANG (measuring the percentage of the population that speaks Asian and Pacific Island languages) and stroke mortality in cluster 2. Conversely, the association between ASIAN_LANG and stroke mortality in cluster 1 remains stable, exhibiting a weakly positive trend over time.

The above results suggest that the association between the density of immigrants or Asian and Pacific Islanders and stroke mortality may not be uniform across regions and time periods. It is worth considering that immigrants or Asian and Pacific Islanders who experience a stroke may encounter challenges in accessing timely stroke care if they do not speak English. This language barrier may potentially contribute to an increased risk of stroke-related death in specific regions and during certain time periods ([Shah et al. \(2015\)](#)). However, our findings indicate that their risks with stroke-related death may have diminished from 2010 to 2018. This reduction may be caused by gradual improvements in stroke care for immigrants or Asian and Pacific Islanders in the U.S., particularly in the counties of cluster 2.

5 Dicussion

In this article, we introduce a novel clustering method for regional divisions of U.S. counties based on their longitudinal associations between SDOH and stroke mortality. The

challenges for this task arise from the latent and cluster-specific nature of the associations, which are compounded by their functional and high-dimensional characteristics simultaneously. To tackle these complex structures, we propose an REM algorithm that utilizes a finite mixture of functional linear concurrent models. Our method explores the clustering-invariant sparsity via a FGS-Net penalty within the REM algorithm, allowing for efficient variable selection in functional covariates to identify the most significant associations among all clusters. The effectiveness of our method has been demonstrated via extensive simulations. In the end we apply the proposed method to the SDOH–stroke mortality longitudinal data, facilitating the regional divisions of U.S. counties. This enables the identification of regions for informing SDOH-targeted prevention of stroke mortality.

In the analysis of the SDOH and stroke mortality dataset, our clustering map in Figure 4 provides a novel result for region-division in stroke management, taking into account the similarity among longitudinal associations between SDOH and stroke mortality. These findings indicate that heterogeneity in these associations occurs even within areas that share similar geographical conditions, stroke mortality rates, or economic statuses. Therefore, region divisions based solely on these factors may not be effective for SDOH-based stroke death control. Moreover, we uncover various patterns of longitudinal associations among the two identified clusters of U.S. counties. The dynamics within these associations, including scale, trends, and inflection points, not only provide heuristic information for understanding complex SDOH-stroke mortality associations but also are useful for establishing timely SDOH adjustments in stroke death control.

Our method can be generalized to other clustering tasks, such as time-varying clustering ([Sartório and Fonseca \(2020\)](#)) and spatial smooth clustering ([Li and Sang \(2019\)](#); [Liang et al. \(2021\)](#)). In these applications, we can relax the assumption of fixed cluster membership to accommodate the desired clustering structures. For instance, to implement time-varying clustering, we can allow cluster memberships to change over time within the finite mixture of functional linear concurrent models; for spatial smooth clustering, spatial dependence structures can be integrated into the model of cluster memberships ([Jiang and Serban \(2012\)](#); [Liang et al. \(2021\)](#)). All these extensions can be achieved by modifying the likelihood function in the REM algorithm, tailored to specific research problem of interest. We leave these as future directions for investigation.

References

- Aneiros, G., S. Novo, and P. Vieu (2022). Variable selection in functional regression models: a review. Journal of Multivariate Analysis 188, 104871.
- Benjamin, E. J., P. Muntner, A. Alonso, M. S. Bittencourt, C. W. Callaway, A. P. Carson, A. M. Chamberlain, A. R. Chang, S. Cheng, S. R. Das, et al. (2019). Heart disease and stroke statistics—2019 update: a report from the american heart association. Circulation 139(10), e56–e528.
- Breheny, P. and J. Huang (2015). Group descent algorithms for nonconvex penalized linear and logistic regression models with grouped predictors. Statistics and computing 25(2), 173–187.
- Cai, T. T., J. Ma, and L. Zhang (2019). Chime: Clustering of high-dimensional gaussian mixtures with em algorithm and its optimality. The Annals of Statistics 47(3), 1234–1267.
- Cai, X., L. Xue, and J. Cao (2022). Variable selection for multiple function-on-function linear regression. Statistica Sinica 32(3), 1435–1465.
- Chiou, J.-M. and P.-L. Li (2007). Functional clustering and identifying substructures of longitudinal data. Journal of the Royal Statistical Society Series B: Statistical Methodology 69(4), 679–699.
- Ding, J., V. Tarokh, and Y. Yang (2018). Model selection techniques: An overview. IEEE Signal Processing Magazine 35(6), 16–34.
- Fan, J. and R. Li (2001). Variable selection via nonconcave penalized likelihood and its oracle properties. Journal of the American statistical Association 96(456), 1348–1360.
- Frieden, T. R. et al. (2013). Cdc health disparities and inequalities report-united states, 2013. foreword. MMWR supplements 62(3), 1–2.
- Gebreab, S. Y., S. K. Davis, J. Symanzik, G. A. Mensah, G. H. Gibbons, and A. V. Diez-Roux (2015). Geographic variations in cardiovascular health in the united states: contributions of state-and individual-level factors. Journal of the American Heart Association 4(6), e001673.
- Ghosal, R., A. Maity, T. Clark, and S. B. Longo (2020). Variable selection in functional linear concurrent regression. Journal of the Royal Statistical Society Series C: Applied Statistics 69(3), 565–587.

- Goldsmith, J. and J. E. Schwartz (2017). Variable selection in the functional linear concurrent model. Statistics in medicine 36(14), 2237–2250.
- Grömping, U. (2007). Relative importance for linear regression in r: the package relaimpo. Journal of statistical software 17, 1–27.
- Havranek, E. P., M. S. Mujahid, D. A. Barr, I. V. Blair, M. S. Cohen, S. Cruz-Flores, G. Davey-Smith, C. R. Dennison-Himmelfarb, M. S. Lauer, D. W. Lockwood, et al. (2015). Social determinants of risk and outcomes for cardiovascular disease: a scientific statement from the american heart association. Circulation 132(9), 873–898.
- He, J., Z. Zhu, J. D. Bundy, K. S. Dorans, J. Chen, and L. L. Hamm (2021). Trends in cardiovascular risk factors in us adults by race and ethnicity and socioeconomic status, 1999-2018. Jama 326(13), 1286–1298.
- Heyden, S., H. A. Tyroler, G. Heiss, C. G. Hames, and A. Bartel (1978). Coffee consumption and mortality: total mortality, stroke mortality, and coronary heart disease mortality. Archives of Internal Medicine 138(10), 1472–1475.
- Holloway, R. G., R. M. Arnold, C. J. Creutzfeldt, E. F. Lewis, B. J. Lutz, R. M. McCann, A. A. Rabinstein, G. Saposnik, K. N. Sheth, D. B. Zahuranec, et al. (2014). Palliative and end-of-life care in stroke: a statement for healthcare professionals from the american heart association/american stroke association. Stroke 45(6), 1887–1916.
- Howard, G. and V. J. Howard (2020). Twenty years of progress toward understanding the stroke belt. Stroke 51(3), 742–750.
- Huang, J. Z., H. Shen, and A. Buja (2009). The analysis of two-way functional data using two-way regularized singular value decompositions. Journal of the American Statistical Association 104(488), 1609–1620.
- Huang, J. Z., C. O. Wu, and L. Zhou (2002). Varying-coefficient models and basis function approximations for the analysis of repeated measurements. Biometrika 89(1), 111–128.
- Imoisili, O. E. (2024). Prevalence of stroke—behavioral risk factor surveillance system, united states, 2011–2022. MMWR. Morbidity and Mortality Weekly Report 73.
- Jacques, J. and C. Preda (2013). Funchlust: A curves clustering method using functional random variables density approximation. Neurocomputing 112, 164–171.

- Jacques, J. and C. Preda (2014). Model-based clustering for multivariate functional data. Computational Statistics & Data Analysis 71, 92–106.
- James, G. M. and C. A. Sugar (2003). Clustering for sparsely sampled functional data. Journal of the American Statistical Association 98(462), 397–408.
- Jiang, H. and N. Serban (2012). Clustering random curves under spatial interdependence with application to service accessibility. Technometrics 54(2), 108–119.
- Kapral, M. K., P. C. Austin, G. Jeyakumar, R. Hall, A. Chu, A. M. Khan, A. Y. Jin, C. Martin, D. Manuel, F. L. Silver, et al. (2019). Rural-urban differences in stroke risk factors, incidence, and mortality in people with and without prior stroke: The canheart stroke study. Circulation: Cardiovascular Quality and Outcomes 12(2), e004973.
- Karp, D. N., C. S. Wolff, D. J. Wiebe, C. C. Branas, B. G. Carr, and M. T. Mullen (2016). Reassessing the stroke belt: using small area spatial statistics to identify clusters of high stroke mortality in the united states. Stroke 47(7), 1939–1942.
- Keribin, C. (2000). Consistent estimation of the order of mixture models. Sankhyā: The Indian Journal of Statistics, Series A, 49–66.
- Khalili, A. and J. Chen (2007). Variable selection in finite mixture of regression models. Journal of the american Statistical association 102(479), 1025–1038.
- Khalili, A. and S. Lin (2013). Regularization in finite mixture of regression models with diverging number of parameters. Biometrics 69(2), 436–446.
- Komárek, A. and L. Komárková (2013). Clustering for multivariate continuous and discrete longitudinal data.
- Kong, D., K. Xue, F. Yao, and H. H. Zhang (2016). Partially functional linear regression in high dimensions. Biometrika 103(1), 147–159.
- Koton, S., A. L. Schneider, W. D. Rosamond, E. Shahar, Y. Sang, R. F. Gottesman, and J. Coresh (2014). Stroke incidence and mortality trends in us communities, 1987 to 2011. Jama 312(3), 259–268.
- Kowarik, A. and M. Templ (2016). Imputation with the r package vim. Journal of statistical software 74, 1–16.

- Labarthe, D., B. Grover, J. Galloway, L. Gordon, S. Moffatt, T. Pearson, M. Schoeberl, and S. Sidney (2014). The public health action plan to prevent heart disease and stroke: Ten-year update. In Washington, DC: National Forum for Heart Disease and Stroke Prevention.
- Lanska, D. J. and L. H. Kuller (1995). The geography of stroke mortality in the united states and the concept of a stroke belt. Stroke 26(7), 1145–1149.
- Li, F. and H. Sang (2019). Spatial homogeneity pursuit of regression coefficients for large datasets. Journal of the American Statistical Association.
- Li, G., H. Shen, and J. Z. Huang (2016). Supervised sparse and functional principal component analysis. Journal of Computational and Graphical Statistics 25(3), 859–878.
- Liang, D., H. Zhang, X. Chang, and H. Huang (2021). Modeling and regionalization of china’s pm2. 5 using spatial-functional mixture models. Journal of the American Statistical Association 116(533), 116–132.
- Lu, Z. and X. Song (2012). Finite mixture varying coefficient models for analyzing longitudinal heterogenous data. Statistics in medicine 31(6), 544–560.
- Mawhorter, S., E. M. Crimmins, and J. A. Ailshire (2023). Housing and cardiometabolic risk among older renters and homeowners. Housing studies 38(7), 1342–1364.
- McNicholas, P. D. and T. B. Murphy (2010). Model-based clustering of longitudinal data. Canadian Journal of Statistics 38(1), 153–168.
- Meier, L., S. Van de Geer, and P. Bühlmann (2009). High-dimensional additive modeling. The Annals of Statistics 37(6B), 3779–3821.
- Morris, J. S. (2015). Functional regression. Annual Review of Statistics and Its Application 2(1), 321–359.
- Mozaffarian, D., E. J. Benjamin, A. S. Go, D. K. Arnett, M. J. Blaha, M. Cushman, S. De Ferranti, J.-P. Després, H. J. Fullerton, V. J. Howard, et al. (2015). Heart disease and stroke statistics—2015 update: a report from the american heart association. circulation 131(4), e29–e322.
- Peel, D. and G. MacLahlan (2000). Finite mixture models. John & Sons.
- Peng, J. and H.-G. Müller (2008). Distance-based clustering of sparsely observed stochastic processes, with applications to online auctions. The Annals of Applied Statistics 2(3), 1056 – 1077.

- Perperoglou, A., W. Sauerbrei, M. Abrahamowicz, and M. Schmid (2019). A review of spline function procedures in r. BMC medical research methodology 19, 1–16.
- Powell-Wiley, T. M., Y. Baumer, F. O. Baah, A. S. Baez, N. Farmer, C. T. Mahlobo, M. A. Pita, K. A. Potharaju, K. Tamura, and G. R. Wallen (2022). Social determinants of cardiovascular disease. Circulation research 130(5), 782–799.
- Ramsay, J. and B. Silverman (2005). Functional Data Analysis (2nd ed.). Springer.
- Ramsay, J. O. and B. W. Silverman (2002). Applied functional data analysis: methods and case studies. Springer.
- Rand, W. M. (1971). Objective criteria for the evaluation of clustering methods. Journal of the American Statistical association 66(336), 846–850.
- Record, N. B., D. K. Onion, R. E. Prior, D. C. Dixon, S. S. Record, F. L. Fowler, G. R. Cayer, C. I. Amos, and T. A. Pearson (2015). Community-wide cardiovascular disease prevention programs and health outcomes in a rural county, 1970-2010. Jama 313(2), 147–155.
- Reshetnyak, E., M. Ntamatungiro, L. C. Pinheiro, V. J. Howard, A. P. Carson, K. D. Martin, and M. M. Safford (2020). Impact of multiple social determinants of health on incident stroke. Stroke 51(8), 2445–2453.
- Rodgers, J., B. A. Briesacher, R. B. Wallace, I. Kawachi, C. F. Baum, and D. Kim (2019). County-level housing affordability in relation to risk factors for cardiovascular disease among middle-aged adults: The national longitudinal survey of youths 1979. Health & place 59, 102194.
- Sartório, V. S. and T. C. Fonseca (2020). Dynamic clustering of time series data. arXiv preprint arXiv:2002.01890.
- Shah, B. R., N. A. Khan, M. J. O'Donnell, and M. K. Kapral (2015). Impact of language barriers on stroke care and outcomes. Stroke 46(3), 813–818.
- Skolarus, L. E., A. Sharrief, H. Gardener, C. Jenkins, and B. Boden-Albala (2020). Considerations in addressing social determinants of health to reduce racial/ethnic disparities in stroke outcomes in the united states. Stroke 51(11), 3433–3439.
- Son, H., D. Zhang, Y. Shen, A. Jaysing, J. Zhang, Z. Chen, L. Mu, J. Liu, J. Rajbhandari-Thapa, Y. Li, et al. (2023). Social determinants of cardiovascular health: a longitudinal

- analysis of cardiovascular disease mortality in us counties from 2009 to 2018. Journal of the American Heart Association 12(2), e026940.
- Tang, X. and A. Qu (2016). Mixture modeling for longitudinal data. Journal of Computational and Graphical Statistics 25(4), 1117–1137.
- Tsao, C. W., A. W. Aday, Z. I. Almarzooq, A. Alonso, A. Z. Beaton, M. S. Bittencourt, A. K. Boehme, A. E. Buxton, A. P. Carson, Y. Commodore-Mensah, et al. (2022). Heart disease and stroke statistics—2022 update: a report from the american heart association. Circulation 145(8), e153–e639.
- Tsao, C. W., A. W. Aday, Z. I. Almarzooq, C. A. Anderson, P. Arora, C. L. Avery, C. M. Baker-Smith, A. Z. Beaton, A. K. Boehme, A. E. Buxton, et al. (2023). Heart disease and stroke statistics—2023 update: a report from the american heart association. Circulation 147(8), e93–e621.
- Varin, C., N. Reid, and D. Firth (2011). An overview of composite likelihood methods. Statistica Sinica, 5–42.
- Villablanca, A. C., C. Slee, L. Lianov, and D. Tancredi (2016). Outcomes of a clinic-based educational intervention for cardiovascular disease prevention by race, ethnicity, and urban/rural status. Journal of Women’s Health 25(11), 1174–1186.
- Wang, J.-L., J.-M. Chiou, and H.-G. Müller (2016). Functional data analysis. Annual Review of Statistics and its application 3(1), 257–295.
- Wang, L., G. Chen, and H. Li (2007). Group scad regression analysis for microarray time course gene expression data. Bioinformatics 23(12), 1486–1494.
- Wang, L., H. Li, and J. Z. Huang (2008). Variable selection in nonparametric varying-coefficient models for analysis of repeated measurements. Journal of the American Statistical Association 103(484), 1556–1569.
- Wang, X., L. Y.-F. Liu, and H. Zhu (2023). Functional finite mixture regression models. Statistica Sinica 33(3).
- Yao, F., Y. Fu, and T. C. Lee (2011). Functional mixture regression. Biostatistics 12(2), 341–353.
- Yao, F., H.-G. Müller, and J.-L. Wang (2005). Functional linear regression analysis for longitudinal data.

- Yi, X. and C. Caramanis (2015). Regularized em algorithms: A unified framework and statistical guarantees. Advances in Neural Information Processing Systems 28.
- Zelko, A., P. R. Salerno, S. Al-Kindi, F. Ho, F. P. Rocha, K. Nasir, S. Rajagopalan, S. Deo, and N. Sattar (2023). Geographically weighted modeling to explore social and environmental factors affecting county-level cardiovascular mortality in people with diabetes in the united states: A cross-sectional analysis. The American Journal of Cardiology 209, 193–198.
- Zeng, L. and J. Xie (2014). Group variable selection via scad-l 2. Statistics 48(1), 49–66.
- Zhou, H., F. Yao, and H. Zhang (2023). Functional linear regression for discretely observed data: from ideal to reality. Biometrika 110(2), 381–393.
- Zhu, H., R. Li, and L. Kong (2012). Multivariate varying coefficient model for functional responses. Annals of statistics 40(5), 2634.
- Zou, H. and T. Hastie (2005). Regularization and variable selection via the elastic net. Journal of the royal statistical society: series B (statistical methodology) 67(2), 301–320.
- Zou, H. and H. H. Zhang (2009). On the adaptive elastic-net with a diverging number of parameters. Annals of statistics 37(4), 1733.